

# Power Management and Control of Common DC Bus Voltage of an Islanded DC Microgrid

Roshan Thakur, Anurendra Singh, Prabhat Dwivedee

**Abstract:** This work deals with system integration and controller design for power management of an islanded DC Microgrid. As the solar and wind power is available for free of cost and as it is also environment- friendly so we can extract the maximum power that is available from these renewable sources. To develop a standalone power generation of a DC micro-grid a combination of Photovoltaic, Wind, Battery storage is connected to a different nature of ac networks connected by a bidirectional converter. By keeping the DC Link voltage constant at its reference value the advantages are that the output ac voltage of the inverter can be kept constant irrespective of variations in the wind speed, solar irradiance, and load. The effectiveness of the control strategy can be tested by applying it to three different natures of load under varying environmental conditions. A permanent magnet synchronous generator (PMSG) based wind energy system (WES) implemented as an energy source. In this paper, the MPPT techniques used are Perturb and Observe (PO) and Hill climb search (HCS) methods are used for WES and PV system respectively. The MPPT is used to extract the maximum power that is available from a renewable source to improve the overall system efficiency. The Battery is used as an energy storage device in this islanded DC microgrid to reduce fluctuation and improves reliability in PV/Wind system due to varying atmospheric conditions. The common DC Bus voltage is also maintained constant so that the local loads on the common DC bus are fed with a constant voltage profile.

**Keywords:** Islanded dc microgrid, photovoltaic array, wind energy system, battery storage system, MPPT.

## I. INTRODUCTION

As the demand of electrical energy is increasing at a very fast rate so to meet the demand we need new sources of electrical energy generation. As the fossil fuels are not going to last for more than 100 years from now so we need to move on to some other alternative sources of clean energy. The fossil fuels is having a negative impact on our environment as the burning of coal for power generation is producing pollution.[1]. And this as causes some of the serious problems like global warming, ecosystem changes, rising sea levels, dying coral reefs. The temperature of the earth is rising due to global warming due to which the oceans are also melting at a fast rate. So the need of the hour is to move on to some other alternative source of energy which are eco-friendly and which do not harm the environment. Some of the various renewable sources which are available are solar, wind, biomass, tidal, geothermal. Out of these available sources the wind and solar are the most abundant in nature.[2] But the problem associated with these are varying nature and dependency on the weather conditions. In order to overcome these limitation we need to connect a battery storage element. The battery used in this paper is Nickel Metal Hydride battery. The NiMh

battery has the advantage that it has 30-40% more capacity as compared to a standard Ni-Cd battery, transportation and storage is easy, environment friendly, recyclable.[3] A microgrid can be defined as power cluster of distributed generation, load, and energy storage device accumulated together in the vicinity to each other. The idea of merging small variable nature sources with energy storage system and controllable loads into flexible entities that are called microgrid. The microgrid can be operated in two modes 1) Grid connected mode 2) Islanded mode. Grid connected mode has several advantages like high efficiency, high reliability.[4] Islanded can be used at places where grid connectivity is not available, in case of disturbances on the main grid, micro grids could potentially disconnect and continue to operate separately, and there are many places on globe in which fossil fuels are not readily available but solar and wind power is easily available in abundance so at these places we can operate in islanded mode operation. There are also several advantages associated with DC Microgrid like higher reliability, no reactive power, reduction in losses, higher efficiency, simpler connection with DC bus, no need of synchronization, no frequency aspect, future DC homes-DC loads such as LED, TV, laptop, dryer, washer and electrical vehicle. In the paper we develop a standalone power generation of a DC micro-grid a combination of Photovoltaic, Wind, Battery storage is connected to a different nature of ac networks connected by a bidirectional converter.[5] The model is tested under varying environmental conditions, along with three different nature of ac load.

## II. MODEL ARCHITECTURE

The DC microgrid used for analysis in this paper which consist the following elements:

- i. DC bus which integrates renewable sources, storage components with the local loads.
- ii. PV module with the boost converter under varying irradiation and temperature.
- iii. Wind energy system consists of 6kW PMSG. The advantage of the PMSG is that it does not need frequent maintenance due to gearless wind rotor and generator [6].
- iv. 300V Battery is integrated to the DC bus via buck boost converter.
- v. Varying three phase load integrated to the DC bus through Inverter.

Power generation and consumption is the continuous process in the microgrid. Hence, there should be power balance in the microgrid. Equation (2.1) explains the power balance among sources, loads and ESSs.

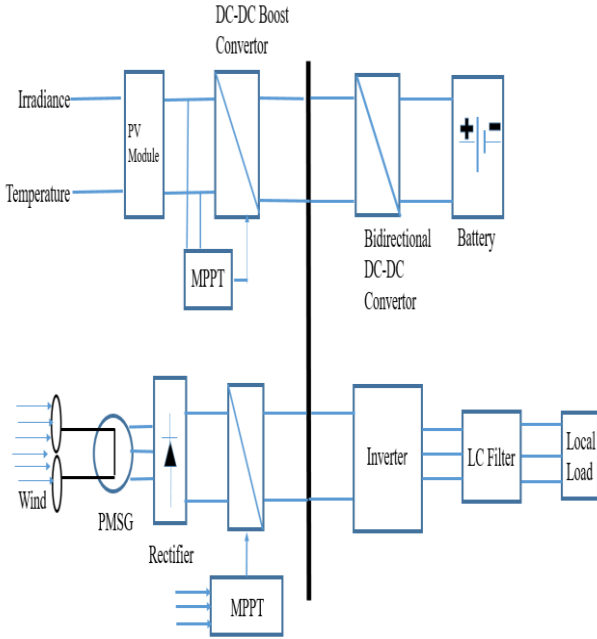


Fig 2.1 Components of DC Microgrid

$$P_{ESS} = P_{DG} - P_{LOAD} \quad (2.1)$$

Where,  $P_{ESS}$  = Power of energy storage system

$P_{DG}$  = Power of distributed generator  $P_{LOAD}$  = Power consumption by load.

### III. Modelling of Various Components

#### 3.1 PV Array Modelling

Modelling pv cell is revealed in the figure below  $R_s$  is located to be in series with the combination of  $R_p$ , diode, and  $I_{ph}$  which collectively are united in parallel.[7]

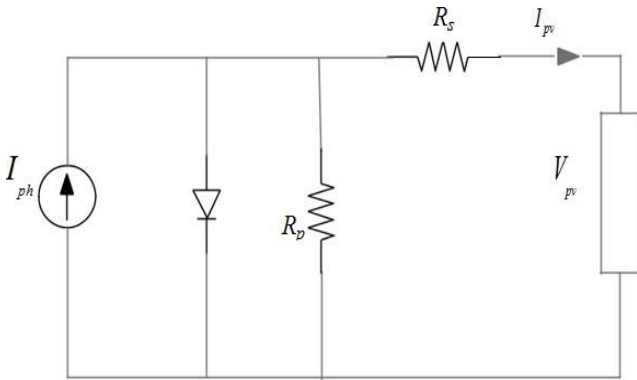


Figure 3.1 PV Cell Diagram

The governing equation for above mentioned cell,

$$I = I_{PV} - I_s \left[ e^{\frac{V+R_s I}{V_T a}} - 1 \right] - \frac{V+R_s I}{R_{sh}} \quad (3.1)$$

$I_{pv}$  = PV Current

$V_T$  = Thermal generated voltage of pv and its value is,

$$V_T = \frac{n K T}{q} \quad (3.2)$$

Where,  $n$ = quantity of cells in series.

$q$  = electron charge.

$T$  = Temperature in Kelvin.

$K$  = Boltzmann constant.

#### 3.1.1 Perturb and Observe Method

As we know that the  $V$  vs  $I$  curve it continuously shifts the maximum power point with the changes with occurs in the irradiance and temperature. So we need a tracker which can track a whole day operation. In the perturb and observe algorithm the first step is to create a perturb in the voltage and current then according to the perturbation the power is being calculated  $p(k)=v(k)*i(k)$  where  $k$  is the number of perturb. If it is found that power is increasing with increase in perturb then we go on increasing the perturbation. At some instant of time when the power attains its maximum point then if we increase the perturbation the power decreases at that instant the perturbation reverses. So we can see that this algorithm perturb around the maximum point. Hence the perturbation size is kept very small in order to have small power variations.[8]

The power which is filed in the  $k+1$  moment is subtracted from the state at  $k$  instant. From the  $V$  vs  $I$  curve it can be perceived that if the curve progresses towards the right then the grade for the  $dP/dV < 0$  and if the curve progresses towards the left side then the  $dP/dV > 0$ . Hence we can recognize that whatsoever is the mark of  $dP[P(k + 1) - P(k)]$  and  $dV[V(k + 1) - V(k)]$  next to subtraction the algorithm chooses whether to progress or to diminish the reference voltage.

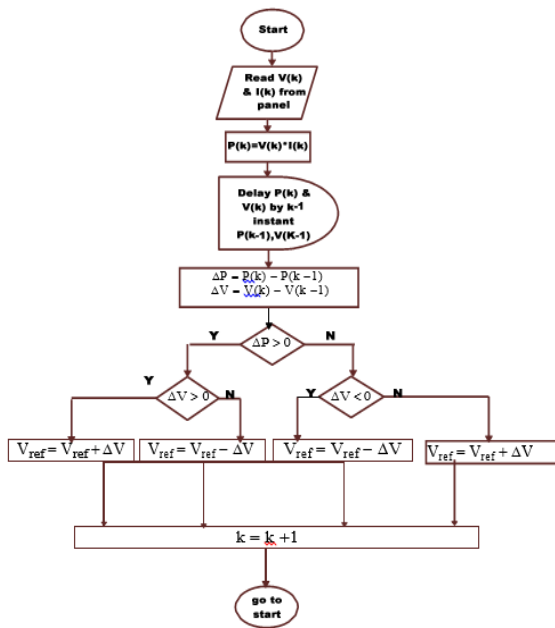


Figure 3.2 Layout of Perturb and Observe

### 3.2 Wind Model

The imminent concerns because of global warming, environmental contamination, and potential security have intensified matter in advancing renewable and environmentally beneficial energy sources such as wind, solar. Wind energy can result in suitable answers to global atmosphere change and power pressure. The utilization of wind power typically drops the emissions of CO<sub>2</sub>, SO<sub>2</sub>, NO<sub>x</sub>, and other adverse wastes as in legendary coal-fuel power plants or radioactive wastes in nuclear power plants.[9]

Wind power Output- The expression for the turbine output power is given by

$$P_T = \frac{1}{2} \rho * A * V^3 \quad (3.3)$$

Where,  $\rho$ = Air density (kg/m<sup>3</sup>)

A= Swept Area (m<sup>2</sup>)

V = Wind velocity (m/s)

#### Wind Control

We are going to use the HCS algorithm to footprint the supreme power. HCS algorithm (neighbourhood exploration, selfish hunt, no posterior trace)

Steps of HCS:

1. Assess the primary state loop unto an explication is fodder or there is not operator left.
2. Choose and employ a distinct operator
3. Appraise the fresh state
4. If intention then halt
5. If more trustworthy than the prevailing state then it is an innovative current status.

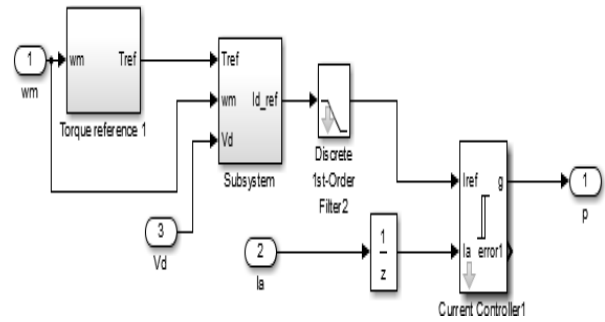


Figure 3.3 Simulink of HCS Controller

Variable speed HCS controller is used to obtain maximum power as shown above. The wind speed is used to produce the reference torque. Then this reference torque along with the voltage of rectifier and wind speed is used to generate the reference current which is given to the current controller. It is matched with the reference current<sup>2</sup> at PMSG and deviation is used to generate the firing pulses for the boost controller. [10,11]

### 3.3 Battery Controller

The voltage of dc bus is compared with the reference battery voltage. Then this difference is passed through a PI controller which used to generate current reference. Then this current is passed through a limiter so that the current remains in a certain limit. Now this reference current is compared with the actual battery current which is then passed through a hysteresis block. The SOC of this battery is then compared with the reference value of 80% if the battery voltage is more than 80% then the battery is not allowed to charge. Then the output of both the hysteresis block and the comparator is given to the product block. If gate pulse Q<sub>2</sub> is triggered then the battery starts charging and if Q<sub>1</sub> is triggered then the battery starts discharging. [12]

The layout of the control is shown below,

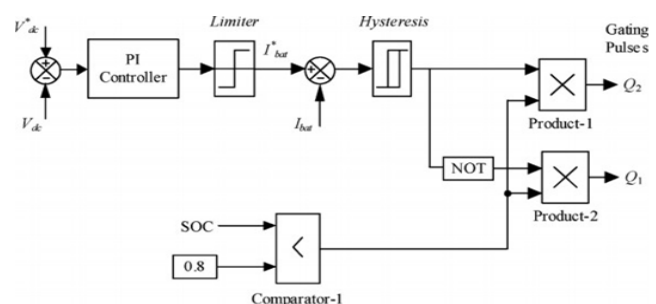


Figure 3.4 Battery Control

### 3.4 Inverter Control

For the proper working of the inverter, the gate pulses should be generated accurately. So we are progressing to first address the GFU.

#### 3.4.1 Traditional GFU

The commutation voltage, is  $V_{com} = \sin(\omega_1 t + \theta_1)$ , which is multiplied by a feedback signal,  $V_{cos} = \cos(\omega_2 t + \theta_2)$ . The output  $V_{error}$  is obtained according to equation 3.5.

$$V_{error} = \sin(\omega_1 t + \theta_1) * V_{cos} = \cos(\omega_2 t + \theta_2) \quad (3.5)$$

$$V_{error} = 0.5 \sin([\omega_1 - \omega_2]t + (\theta_1 - \theta_2)) + 0.5 \sin([\omega_1 + \omega_2]t + (\theta_1 + \theta_2)) \quad (3.6)$$

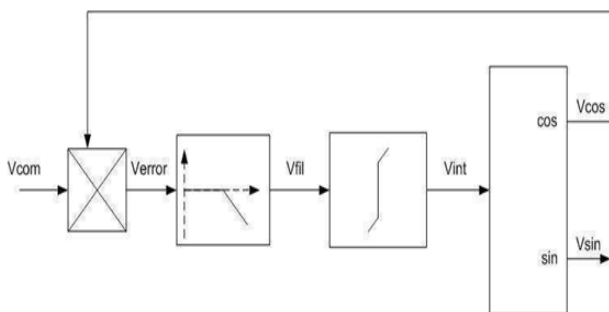


Figure 3.5 Block of GFU

The first term of above equation outlines the error among the voltage synchronizing and the voltage commutation due to the difference of phase and frequency. When the voltage commutation is locked with synchronizing voltage then  $\omega_1 = \omega_2$ ,  $\theta_1 = \theta_2$  are alike. The second term is undesired ac segment which possesses frequency of  $2\omega_1$ . To remove the dc error signal and to filter out the unwanted ac segment, the transfer function  $\omega c / (s + \omega c)$  of the low-pass filter is employed. Output is passed upon an integrator with a transfer function of  $1/sT_i$ . Integrator output,  $V_{int}$ , is utilized to change the frequency and phase of a free-running Sine-Cosine Oscillator to generate output signal  $V_{sync}$ . Under Steady-state, these feedback signal  $V_{sync}$  will be in same phase and frequency as  $V_{com}$  commutation voltage. Thus,  $V_{sync}$  could be employed as a stable pollution-free signal to derive zero-crossover points to provide the timing reference points for the GFU.[13]

#### 3.4.2 DQO GFU

The DQO GFU is depicted in Figure 3.6

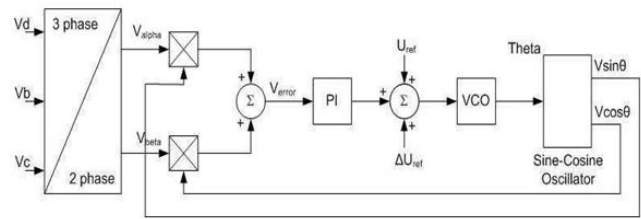


Figure 3.6 Block diagram of DQO GFU

The DQO GFU equations mentioned below,

$V_a, V_b$  and  $V_c$  are the voltages of the 3 phase.

The  $V_{error}$  is the error in voltage. The voltage  $\theta$ . The  $V_{sync}$  synchronizing voltage and  $V_{com}$  commutation voltage.

We obtain DQO axis 2 components as  $V_{beta}$  and  $V_{alpha}$  these are obtained from  $V_a, V_b$  and  $V_c$  the commutation voltages of 3 phase by utilizing the equations 3.3 and 3.8,

$$V_{beta} = \frac{1}{\sqrt{3}} (V_b - V_c) \quad (3.7)$$

$$V_{alpha} = \frac{2}{\sqrt{3}} V_a - \frac{1}{3} V_b - \frac{1}{3} V_c \quad (3.8)$$

$$V_{error} = (V_{alpha} V \sin \theta) + (V_{beta} V \cos \theta) \quad (3.9)$$

An error signal,  $V_{error}$ , derived using equation 3.9, is fed through a PI controller to generate a reference value for the VCO. This reference value can be modulated by a signal  $\Delta U_{ref}$ , and it has a fixed voltage bias  $U_{ref}$  which sets the center frequency of the VCO. The output of the VCO is a signal proportional to a saw tooth waveform. This waveform is used to generate the Sine-Cosine waveforms which are fed back to the multipliers to generate the error signal. [14]

Under steady state, this error is reduced to zero and the output of the Sine-Cosine oscillator will be in synchronism with the commutation voltages.

The small signal block diagram of the DQO grid control unit is shown in Figure 3.7, where

$$G(s) = K_{pi} (1 + s T_{pi}) / s T_{pi} \quad (3.10)$$

represents the PI transfer function. The loop transfer function is given in equation 3.11.

$$T(s) = K_{pi} (1 + s T_{pi}) / s T_{pi} * (1 / s T_{pi}) \quad (3.11)$$

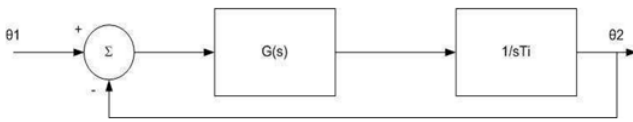


Figure 3.7 Block Diagram of DQO grid unit

### 3.4.3 Synchronization techniques

Firing pulse creation unit of the static converter significantly affects the transient performance of the converter. The VCO related to PLL is utilized to produce firing pulses equidistant an satisfactory transient presentation can be accomplished even with the generally feeble AC framework. The utilization of VCOs to the firing control converter, this strategy drives equidistance terminating pulses for the converter valves and to a large extent, decoupled the effect of any AC voltage distortion on the valve triggering.”[15] “One normal kind of GFU referred to as the Conventional sorts depend on a VCO related to PLL. In the circuit, the synchronizing voltage  $V_{sync}$  is compared and the  $V_{com}$  commutation voltage from the ac system bus. The error between these two signal is then fed to a VCO to change the phase and the frequency of the synchronizing voltage such that this error is reduced to zero.[16]

### 3.4.4 PWM Inverter Controller

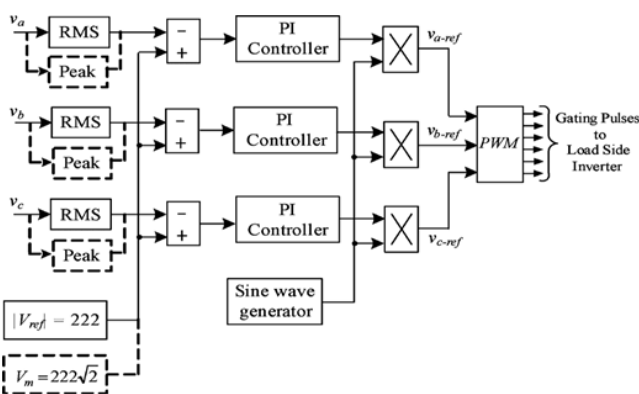


Figure 3.8 PWM Inverter Controller

The three phase voltages on the ac side are compared with the reference voltages of each phase. Then the mismatch which is been generated is feed to a PI controller which is used to reduce the error. Then this output is multiplied with a sine wave generator. This is used to generate the reference value

for the three phases. Then these reference voltages are feed to a discrete PWM generator. This is then used to produce gate pulses for firing the inverter. [17]

### 3.4.5 Control of Power

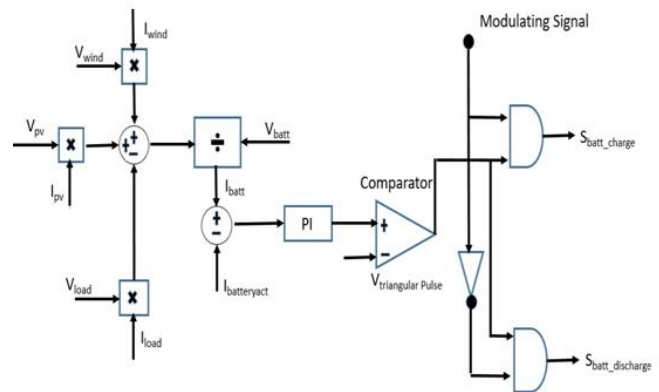


Figure 3.9 Power Control Block

For the management of the power the method which has been employed is denoted above in the figure. The power is obtained by the multiplication of the input of voltage and current that is coming from the solar. The in a similar fashion by considering the wind voltage and current the wind power is being calculated. Then these two powers are added up. This added power will result in the total power which renewable sources can deliver. Then the total renewable power is deducted from the essential load power. So we get the whole mismatch in the power. This mismatch power is divided with nominal battery voltage which has been admitted as 300V. Then we get the reference battery current. Then this reference battery current is subtracted with the real current which is passing battery. This difference in the current is permitted to pass into a PI controller. Then this output is matched in a comparator with a carrier signal of frequency 5.5 KHz to create the pulses for the control of battery converter. The output of the AND gate is used to decide the mode of operation of the bidirectional DC-DC converter. The modulating signal and the resultant of the comparator are the inputs to the AND logic gate. When the renewable sources are having more power than the required load power the bidirectional converter operate in buck mode. And value that is present at the modulating signal is 1. And in this circumstance, the battery starts charging and load is supplied power by the renewable sources.

Considering the case meanwhile the load power is extended numerous than renewable formed power then in that case the bidirectional converter functions in boost mode. And the value which is present at the modulating signal is 0. In this circumstance, the load is supplied from renewable sources and battery both. So the battery starts discharging.[18]

**IV. Simulation Results**

The Simulink model used in this paper is given below,

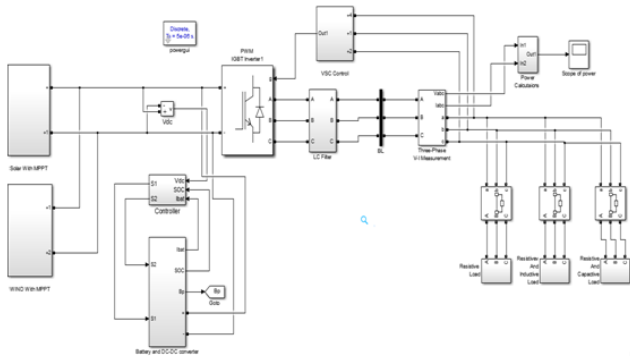


Figure 4.1 Simulink Block of DC Microgrid

DC microgrids constructed above consist of three different nature of load.

Various types of Loads

- 1) A resistive load The active power required is 45 KW.
- 2) A resistive and inductive load. The active power required is 55 KW and reactive power required is 10 KW.
- 3) A resistive and capacitive load. The active power required is 66 KW and reactive power required is 10 KW. Three cases are taken into consideration,

Case1:  $0 < t < 2$  sec

Status of Circuit breaker Circuit Breaker 1-closed, 2-open, 3-open.

A resistive load is connected to the microgrid and during this time wind power is negligible only PV power is present. The load active power requirement is 45 KW but the PV generates 65 KW. So the battery is getting charged during this time period.

Case2:  $2 < t < 4$  sec

Status of Circuit breaker

Circuit Breaker 1-closed, 2-closed, 3-open.

A resistive and inductive load is connected to the microgrid. Total active power requirement is 55 KW and reactive power

requirement is 10KVAR. The PV is able the produce 29 KW. The wind is able to produce 6 KW. So the battery is getting discharged during this time period and giving 20KW.

Case3:  $4 < t < 6$  sec

Status of Circuit breaker

Circuit Breaker 1-closed, 2-open, 3-closed.

A resistive and capacitive load is connected to the microgrid. Total active power requirement is 66 KW and reactive power requirement is 10KVAR. The PV is able the produce 52 KW and the wind is able to produce 4 KW. So the battery is getting discharged during this time period and giving 10KW so that the generation meets the demand. Here as the penetration of DG is more so the battery is required to discharge less.

Now the Simulink model and the Matlab results have been discussed for all the components.

**4.1 Simulink model of the PV Array**

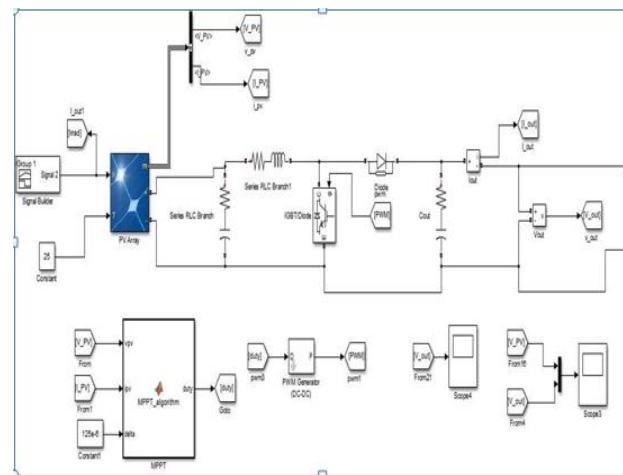


Figure 4.2 Simulink Model of PV with boost converter.

In the block an variable irradiancie and variable temperature is given as input to PV array. Then the output voltage is boosted up by the boost converter. The firing pulse of the boost converter is controlled by the mppt algorithm.

The values which have been used for the boost Converter is illustrated below, Value of Inductor is  $2 \times 10^{-3}$ . Value of capacitor is  $100 \times 10^{-6}$ .

The figure of the varying irradiancie is shown below,

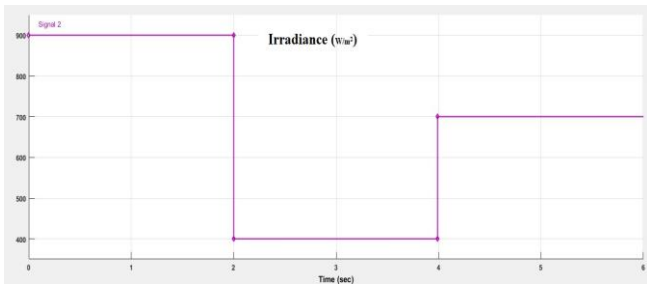


Figure 4.3 Irradiance Input to the PV panel

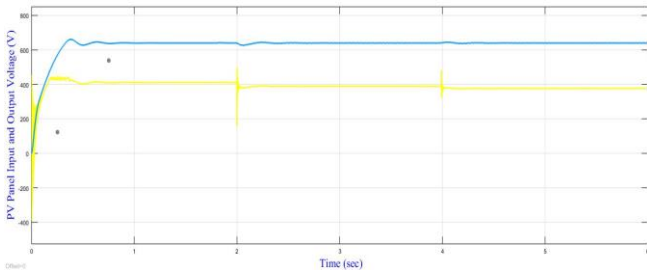


Figure 4.4 Input and output voltage at the PV panel

We can make an observation from the above graph that the voltage value at the input panel is having a slight fluctuating value around 400V but with the use of boost Converter and MPPT algorithm which in this case is perturb and observe we can figure out that the voltage gets rise up to a value of 640V.

#### 4.2 Simulink model of the Wind

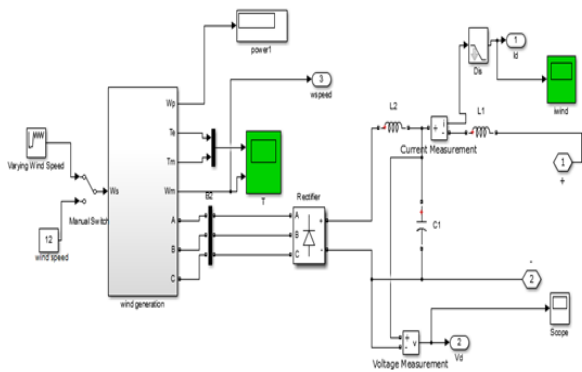


Figure 4.5 Simulink Model of Wind Model

The PMSG turbine has been considered. As the output of the wind is changing innature so we have taken rectifier to get dc output voltage. The wind speed is having a variable speed for 0-6 sec.

The input voltage which has been generated is show,

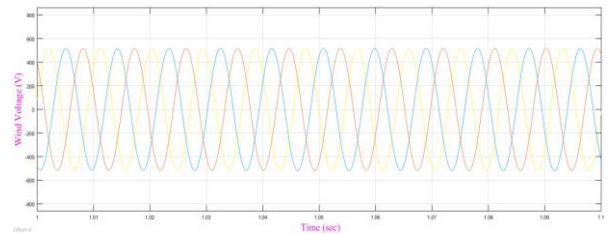


Figure 4.6 Input Voltage of Wind

We can observe that a sinusoidal voltage is being generated by the wind.

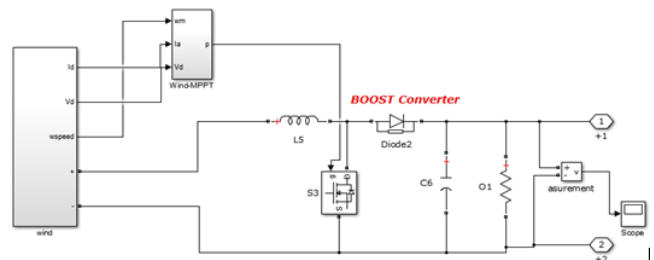


Figure 4.7 Simulink of wind connected to boost Converter

The Simulink diagram of the boost Converter used for wind model is shown above. The firing of the boost is controlled by the HCS algorithm. And this voltage is then feed to the DC bus.

The value of the parameters of the Converter is given below,

Inductor value is  $100 \times 10^{-6}$  and Capacitor value is  $100 \times 10^{-3}$ .

The input to the boost Converter and the output is shown below,



Figure 4.8 Wind Input and Output Voltage

We can make an observation from the above figure that the input voltage is having wide fluctuations but due to the use of the battery we are able to get a constant outputvoltage.

The input moves around 300V to 600V. But the output is not being able to change due to the presence of battery.

### 4.3 Battery Modelling

The model of the battery is shown below,

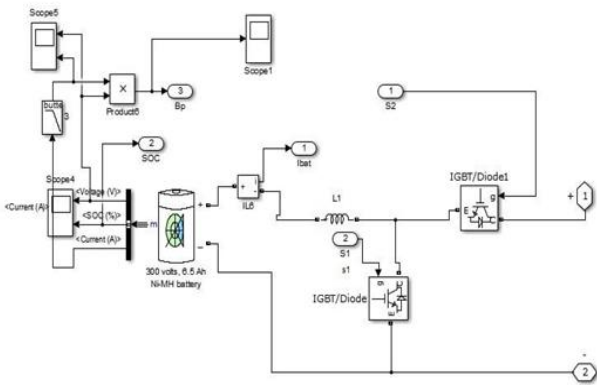


Figure 4.9 Simulink Model of Battery

The waveform for the battery voltage is shown below,

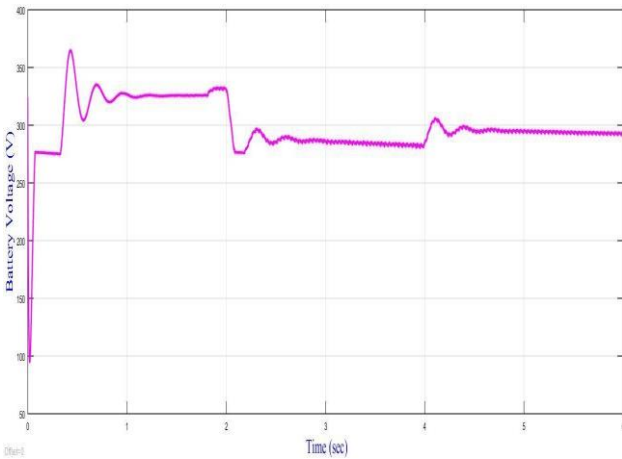


Figure 4.10 Waveform of Battery Voltage

The battery above figure can be discussed for the three loading conditions,

1) From the figure we can observe that during 0-2 sec as the load only the PV is present and the wind is negligible. The DG is able to generate 65KW power but only 45KW of load is present so the battery starts charging from 300V to 325V.

2) Now 0-4sec as the load the PV has 29KW and wind generates 6KW. The DG is able to generate 35KW power but 55KW of load is present so the battery starts discharging from 325V to 285V.

3) Now 0-6sec as the load the PV has 52KW and wind generates 4KW. The DG is able to generate 56KW power but 66KW of load is present so as now the need

for the power needed by battery is less so it discharges till 295V only.

The Current of the Battery is shown below,

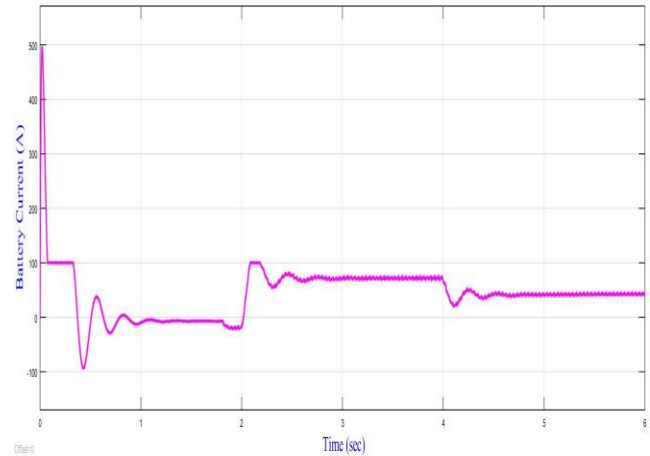


Figure 4.11 Waveform of Battery Current

The DG is able to generate 65KW power but only 45KW of load is present so the battery starts charging and the current is around 6A.

The DG is able to generate 35KW power but 55KW of load is present so the battery starts discharging the current is 72.5A.

The DG is able to generate 58KW power but 66KW of load is present so the current flowing is around 42A.

Now the current and the Voltage of the battery are plotted on the same graph for much clarity.

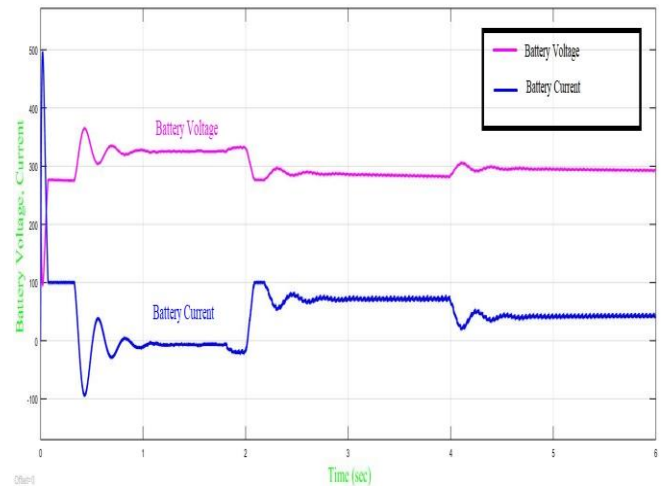


Figure 4.12 Waveform of Battery voltage and current.

The graph for the power delivered by the battery is given below

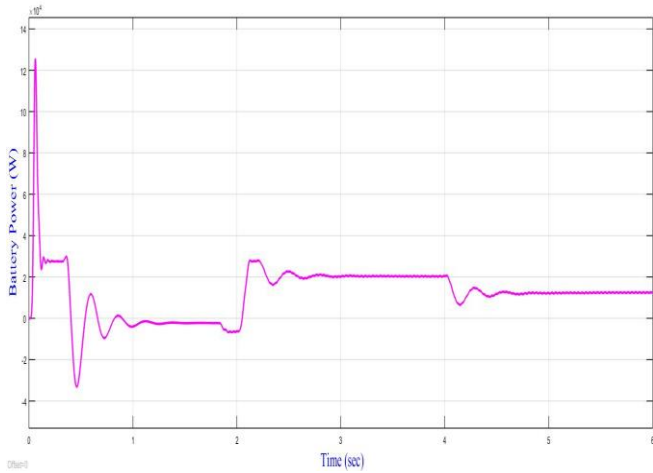


Figure 4.13 Waveform of Battery Power

The DG is able to generate 65KW power but only 45KW of load is present so the battery is getting charged.

The DG is able to generate 35KW power but 55KW of load is present so the battery starts discharging and supplies the rest of 20KW.

The DG is able to generate 58KW power but 66KW of load is present so the battery is discharging at a less rate and has to supply around 8KW.

SOC of the battery is shown below,

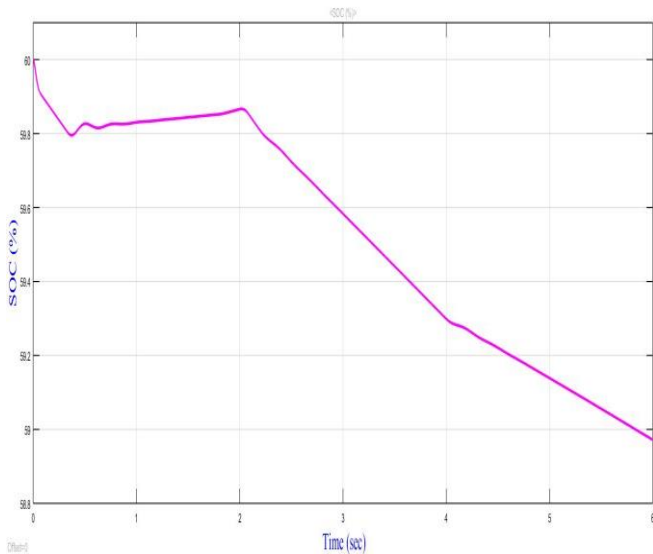


Figure 4.14 SOC of the Battery

SOC in first case which is resistive in at the starting rises from 59.8 to 59.87.

SOC in the second case which is inductive and resistive in nature the load wants 55KW but the DG can only fulfil 35KW so the SOC falls from 59.87 to 59.3.

SOC in the third case which is capacitive and resistive in nature the requirement of load is 66KW and the DG generates 58kw so the battery has to supply a less amount of power as

compared to the above case so the SOC falls from 59.3 further to 58.95.

#### 4.4 Load Waveform

Voltage At load Side

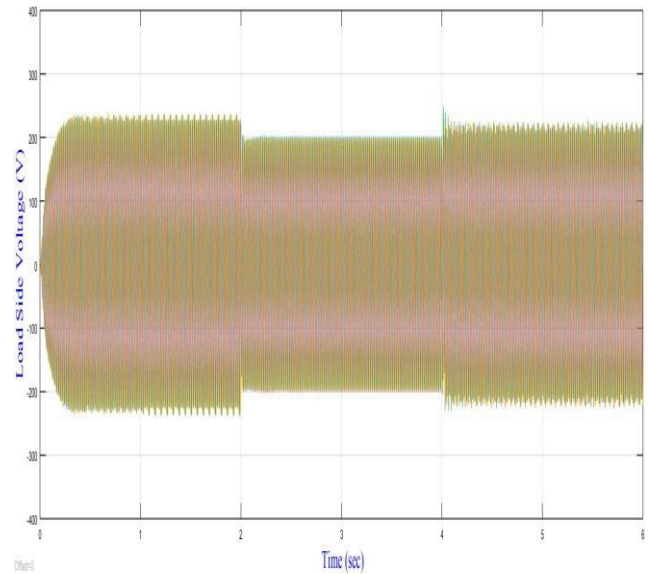


Figure 4.15 Waveform of Load Voltage

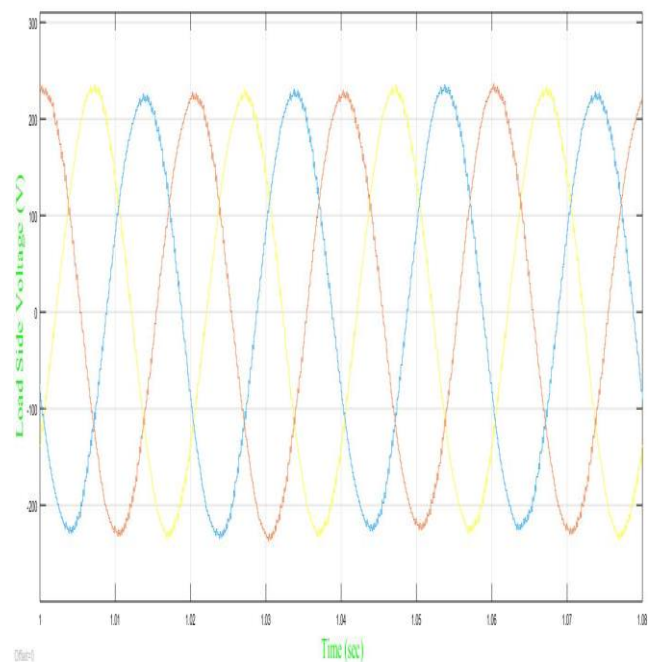


Figure 4.16 Waveform of Load Voltage

The figure are used to show the waveform of Load Voltage. As the load which has been taken into consideration is a three phase load so we are able to get the resultant waveform as a balanced voltage.

4.5 Common DC Bus Voltage

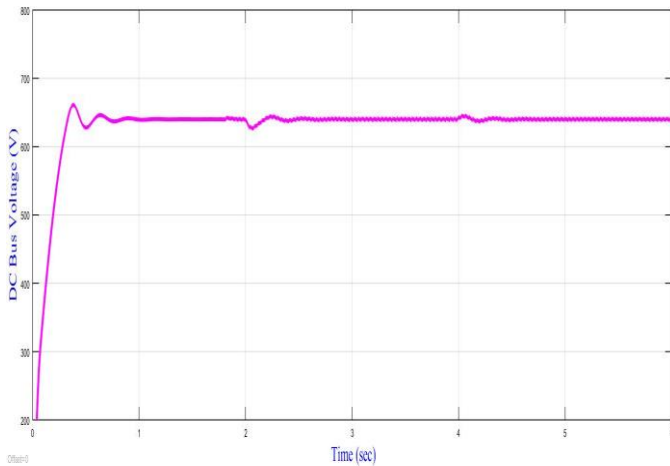


Figure 4.17 Waveform of DC Bus Voltage

As it is mandatory to keep the DC Bus voltage constant so that whatever local load are being satisfied by the DC bus must be able to experience a constant voltage. This is voltage at the common DC Bus from the above figure we can conclude that irrespective of the changes in environmental conditions and changes in the load we can observe that the DC bus voltage is found to be constant in nature. The voltage of 640V is maintained constant at the DC bus.

4.6 Power of all Distributed sources, Battery and Load.

The waveform for the power flow is shown below,

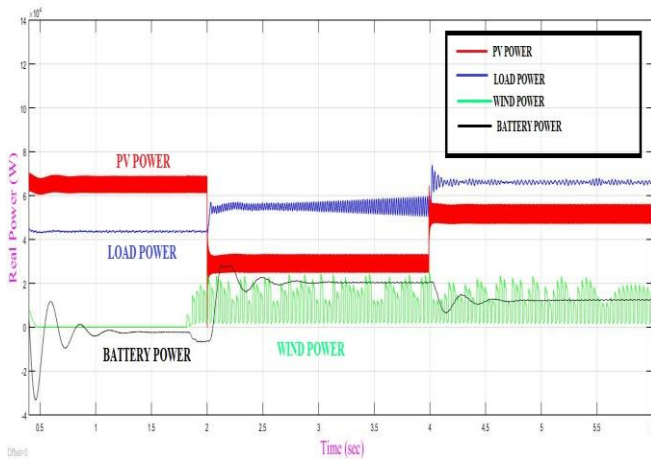


Figure 4.18 Power curve of all Distributed sources, Battery and Load.

So we can finalize the work after watching the above curve the cases are divided in three sections,

Case1:  $0 < t < 2$  sec

For 0-2 sec the requirement of load is 45KW as one we can observe that the energy which wind is giving is zero. So the entire burden comes to PV. But the Capacity of generation of PV is around 65KW. The mode which battery decided is charging and it gets charged up by the 21KW of the left power which is extra.

2) Case2:  $2 < t < 4$  sec

For  $2 < t < 4$  the load is inductive resistive in nature. Net power required is 55KW by load in which the wind has contributed to 6KW and the solar contribution is 29KW. As the DG is not able to fulfil the need so battery decided discharge mode and hence it gives 20KW of active power so that the need can be counter balanced by the wants.

3) Case3:  $4 < t < 6$  sec

For  $4 < t < 6$  the load is capacitive along with resistive in nature. Net power required is 66KW by load in which the wind has contributed to 4KW and the solar contribution is 52KW. As the DG is not able to fulfil the need so battery decided discharge mode and hence it gives 10KW of active power so that the need can be counter balanced by the wants.

V. CONCLUSION

This work exhibits the modelling of a DC microgrid which is in islanded mode. This microgrid which is in islanded mode includes WES, ESS for diminishing the varying nature of the renewable sources and PV. We are able to build a steady Matlab Simulink model of islanded DC microgrid which works for diversifying environmental conditions and also altering nature of the load. We have elaborated the controller for doing the power management of this system. The design for the mppt for both wind and solar has been build so that we are able to harness the maximum power which is been available. The Hill and Climb is used for wind and Perturb and Observe is used for the solar mppt. The islanded grid can provide secure, great quality and increased efficient power to the local consumer. The common DC bus voltage is also held constant so that the local load which are connected to it can experience constant voltage. The controller which is developed for the battery is working efficiently and the proper charge and discharge of the battery is taking place to satisfy the power balance. A stable operating microgrid has been built.

## VI. REFERENCES

- [1] Podder, S., Khan, R.S. and Alam Mohon, S.M.A., 2015. The technical and economic study of solar-wind hybrid energy system in coastal area of Chittagong, Bangladesh. *Journal of Renewable Energy*, 2015.
- [2] Abdullah, M.A., Yatim, A.H.M., Tan, C.W. and Saidur, R., 2012. A review of maximum power point tracking algorithms for wind energy systems. *Renewable and sustainable energy reviews*, 16(5), pp.3220-3227.
- [3] Kopera, J.J., 2004. Inside the Nickel metal hydride battery. Cobasys, MI, USA [http://www.cobasys.com/pdf/tutorial/inside\\_nimh\\_battery\\_technology.pdf](http://www.cobasys.com/pdf/tutorial/inside_nimh_battery_technology.pdf) (Accessed 08/11).
- [4] Strunz, K., Abbasi, E. and Huu, D.N., 2013. DC microgrid for wind and solar power integration. *IEEE Journal of emerging and selected topics in Power Electronics*, 2(1), pp.115-126.
- [5] Eghtedarpour, N. and Farjah, E., 2014. Distributed charge/discharge control of energy storages in a renewable-energy-based DC micro-grid. *IET Renewable Power Generation*, 8(1), pp.45-57.
- [6] Li, S., Haskew, T.A. and Xu, L., 2010. Conventional and novel control designs for direct driven PMSG wind turbines. *Electric Power Systems Research*, 80(3), pp.328-338.
- [7] Ding, F., Li, P., Huang, B., Gao, F., Ding, C. and Wang, C., 2010, September. Modeling and simulation of grid-connected hybrid photovoltaic/battery distributed generation system. In *CICED 2010 Proceedings* (pp. 1-10). IEEE.
- [8] Femia, N., Petrone, G., Spagnuolo, G. And Vitelli, M., 2004, May. Perturb And Observe MPPT Technique Robustness Improved. In *2004 IEEE International Symposium On Industrial Electronics* (Vol. 2, Pp. 845-850). IEEE.
- [9] Muller, S., Deicke, M. and De Doncker, R.W., 2002. Doubly fed induction generator systems for wind turbines. *IEEE Industry applications magazine*, 8(3), pp.26-33.
- [10] Gao, J., Lu, J., Huang, K., Zhang, Y. and Huang, S., 2009, October. A novel variable step hill-climb search algorithm used for direct driven PMSG. In *2009 International Conference on Energy and Environment Technology* (Vol. 1, pp. 511-514). IEEE.
- [11] Li, H., Li, Q., Jiang, X., Ruan, Y. And Huang, W., 2013. The Application Of Improved Hill-Climb Search Algorithm In Wind Power Generation. *IFAC Proceedings Volumes*, 46(20), Pp.263-267.
- [12] Samrat, N.H., Ahmad, N.B., Choudhury, I.A. and Taha, Z.B., 2014. Modeling, control, and simulation of battery storage photovoltaic-wave energy hybrid renewable power generation systems for island electrification in Malaysia. *The Scientific World Journal*, 2014.
- [13] Sood, V.K., Khatri, V. And Jin, H., 1995. Performance Assessment Using Emtp Of Two Grid Firing Units For HvdC Converters Operating With Weak Ac Systems.
- [14] Sood, V.K., 2004. Synchronization Techniques For Power Converters. *HVDC And FACTS Controllers: Applications Of Static Converters In Power Systems*, Pp.39- 66.
- [15] Ainsworth, J.D., 1967, July. Harmonic instability between controlled static converters and ac networks. In *Proceedings of the Institution of Electrical Engineers* (Vol. 114, No. 7, pp. 949-957). IET Digital Library.
- [16] Wolaver, D.H., 1991. Phase-locked loop circuit design. *Organization*, 1, p.7.
- [17] Bhende, C.N., Mishra, S. and Malla, S.G., 2011. Permanent magnet synchronous generator-based standalone wind energy supply system. *IEEE transactions on sustainable energy*, 2(4), pp.361-373.
- [18] Singh, D., Agrawal, A. and Gupta, R., 2017, December. Power Management In Solar PV Fed Microgrid System With Battery Support. In *2017 14th IEEE India Council International Conference (INDICON)* (pp. 1-6). IEEE.

**Roshan Thakur** is Assistant professor in Electrical Engineering Dept. of Bansal Institute of Engineering and Technology Lucknow,U.P,India

**Anurendra Singh** is Assistant professor in Electrical Engineering Dept. of Bansal Institute of Engineering and Technology Lucknow,U.P,India

**Prabhat Dwivedee** Assistant professor in Electrical Engineering Dept. of Prabhat Engineering College Kanpur,U.P,India